International Communications in Heat and Mass Transfer 56 (2014) 63–70

Contents lists available at ScienceDirect

International Communications in Heat and Mass Transfer

journal homepage: www.elsevier.com/locate/ichmt

# Non-invasive estimation of size and location of a tumor in a human breast using a curve fitting technique☆

Koushik Das, Subhash C. Mishra *

*Department of Mechanical Engineering, Indian Institute of Technology Guwahati, Guwahati 781039, India*

ARTICLE INFO

Available online 22 May 2014

*Keywords:*
Pennes bioheat model
Finite volume method
Curve fitting technique
Skin surface temperature
Tumor characteristics
Inverse analysis

ABSTRACT

This article deals with the estimation of the size and location of a tumor in the breast. Estimation is based on the measurement of the skin surface temperature. With skin surface temperature known, the estimation is done using the newly proposed curve fitting technique. For the present study, justification is shown for the consideration of a 2-D geometry of the breast instead of its 3-D hemispherical shape. Heat transfer in a blood perfused tissue is analyzed using the Pennes bioheat equation. The steady-state temperature distribution in the tissue-tumor system is obtained by solving the bioheat equation using the finite volume method. The size and location of the tumor are accurately estimated. Computationally, the procedure is highly efficient.



## 1. Introduction

Modern science has given us the power of performing day-to-day activity with ease and comfort. But, the changed life-style has resulted in one of the biggest threats, the cancer, the humanity is facing. Consumption of tobacco products, unhealthy diet, low physical activity, increasing pollution and adulteration of food, etc. lead to the manifestation of this lethal disease called cancer [1]. Besides these external factors, certain genetic issues also remain the cause of this disease. Such genetic issues increase the risk of the breast and the ovarian cancers.

Breast cancer contributes the most in cancer related deaths in women [2]. As per World Cancer Report — 2008 by WHO, breast cancer accounts for 12.7% of the total cancer related death in women. The number of new cases of breast cancer in the USA alone for the year 2013 in female and male is estimated to be 232,340 and 2240, respectively [1]. Out of which, the expected number of deaths is 39,620 in female and 410 in male. Worldwide, the total number of patients with breast cancer is huge. Hence, any effort towards diagnosis and/or prognosis of the breast cancer is a welcome move.

Mutations of the DNA causes cancer, and unlike normal cells, cancer cells are characterized by its uncontrolled growth forming a lump, called tumor. In the advanced stage, cancer cells get into the circulatory and lymphatic system of the body, and get transported to other organs. Once settled down, they start taking the form of a cancer in that organ too. This happens during its metastasis stage. In a breast, normally a cancer starts in the lobules where milk is produced. But, with its progression, cancer spreads to the milk carrying ducts and the lymphatic glands too. Not all, but in most of the stages of breast cancer, the diameter of a tumor can be as high as 5 cm [3], and under severe conditions, it may even be bigger. Like other diseases, diagnosis comes first in the treatment of cancer too. An early diagnosis means better treatment and better chances of cure. Modern diagnostic medical facilities are equipped with computed tomography (CT) scan and magnetic resonance imaging (MRI), particularly X-ray mammography for the breast tumor. These are associated with high cost of operation and maintenance combined with long duration of procedures, radiation hazard, etc. [4].

A human body generates and convects heat in various ways. Heat transfer remains an important subject in the analysis of a human body. Thus, a human body is nothing but a thermal system. An equation governing the transport of heat in the blood perfused tissue was proposed by Pennes [5–11]. This famous bioheat equation is based on experimental study on the human forearm, in which, in a controlled environment, he invasively measured the temperatures of the tissue. A good number of studies till date are based on Pennes bioheat equation [12–15].

At a particular condition, a tissue in a living body carries distinct thermal and optical signatures. Any change in the conditions of the tissue alters these signatures [16,17]. Growth of a tumor in a body increases the rate of metabolism and changes the blood perfusion rate in the region of its appearance. Due to the changed behavior, a variation in the thermal and optical signals of the tissue is observed. A cancerous tissue has different temperature profile and different temporal transmittance and reflectance signals than that of a healthy tissue. Measurement and analysis of these signatures, open up a way to estimate the presence of any abnormality in the tissue that has caused it [18–20]. Many researchers have observed that, the grade of the abnormality, the location and the size of a tumor in the tissue yields a

☆ Communicated by W.J. Minkowycz.

* Corresponding author.
*E-mail address:* scm_iitg@yahoo.com (S.C. Mishra).

http://dx.doi.org/10.1016/j.icheatmasstransfer.2014.04.015
0735-1933/

**Nomenclature**

| | |
|---|---|
| $A$ | amplitude of temperature profile, °C |
| $c_p$ | specific heat of the tissue, J/kg · K |
| $c_{pb}$ | specific heat of the blood, J/kg · K |
| $k$ | thermal conductivity, W/m · K |
| $L$ | length, cm |
| $Q_m$ | metabolic heat generation, W/m$^3$ |
| $Q_s$ | distributed volumetric heat source due to spatial heating, W/m$^3$ |
| $r$ | radius, cm |
| $t$ | time, s |
| T | temperature, °C |
| $T_a$ | temperature of the artery, °C |
| $T_e$ | local heat source temperature, °C |
| $V$ | volume of the cell, m$^3$ |
| Y | distance of the center of tumor from bottom boundary of the tissue domain, cm |

*Greek symbols*

| | |
|---|---|
| $\eta_b$ | blood perfusion rate, m$^3$/s · m$^3$ |
| $\rho$ | density, kg/m$^3$ |
| $\rho_b$ | density of blood, kg/m$^3$ |

*Subscripts*

| | |
|---|---|
| $E$ | East |
| $N$ | number of control volumes |
| $P$ | cell center |
| $t$ | tumor |
| $W$ | West |

*Superscript*

| | |
|---|---|
| $n$ | time level |

unique thermal signal. Hence, its analysis can be able to reveal various features of the tumor in the tissue [21,22]. With an aim to improve diagnostic procedures of a breast cancer, in the present work, consideration is given to the estimation of the size and the location of a tumor in the breast tissue. The change in the skin surface temperature profile is the basis of estimation. With skin surface exposed to the convective environment, the solution of Pennes bioheat equation using the finite volume method (FVM) provides the temperature profile. Next a curve fitting technique is employed to estimate the size and the location of the tumor.

## 2. Formulation

Fig. 1a shows the schematic of a 2-D (width × depth: 2 $L \times L$) breast tissue with a centrally located tumor. Thermal conditions of the left ($x = 0$, $y$) and the right ($x = 2L$, $y$) boundaries of the tissue are not affected with the presence of the tumor, and are thus adiabatic, i.e., $\left(\frac{\partial T}{\partial x}\big|_{(0,y)} = 0\right)$ and $\left(\frac{\partial T}{\partial x}\big|_{(2L,y)} = 0\right)$. The bottom ($x$, 0) boundary of the tissue is at the core body temperature $T_a$, and it is isothermal ($T|_{(x,0)} = T_a$). The top ($x$, $L$) boundary of the tissue is the surface of the skin, and it is exposed to the convective boundary condition $\left(-k\frac{\partial T}{\partial x}\big|_{(x,y)} = h(T - T_f)\right)$, where $k$ is the thermal conductivity, $h$ is the convective heat transfer coefficient, and $T_f$ is the ambient temperature. Among the four boundaries, effect of the tumor, in terms of temperature rise, is felt only on the north ($x$, $L$) boundary, i.e., the skin surface.

Heat transfer in a blood perfused tissue is governed by Pennes bioheat equation [5,11]. It is given by

$$\rho c_p \frac{\partial T}{\partial t} = \underbrace{k\left(\frac{\partial^2 T}{\partial x^2} + \frac{\partial^2 T}{\partial y^2}\right)}_{I} + \underbrace{\eta_b \rho_b c_{pb}(T_a - T)}_{II} + \underbrace{Q_m}_{III} + \underbrace{Q_s}_{IV} \tag{1}$$

where $\rho$, $c_p$ and $\eta_b$ are the density, specific heat and blood perfusion rate of the tissue, respectively, and $\rho_b$ and $c_{pb}$ are the density and the specific heat of the blood, respectively. $Q_m$ and $Q_s$ represent metabolic heat generation rate and distributed volumetric heat source due to spatial heating, respectively. When a tumor manifests in a tissue, metabolic heat generation rate $Q_m$ and some of the thermo-physical properties like the blood perfusion rate $\eta_b$ of the tissue are altered. The change in these parameters results in changed skin surface temperature. For a healthy tissue, the skin temperature remains constant, however, a tumor that acts like a localized heat source within a tissue, causes spatial variation in the skin surface temperature.

An observation of Eq. (1) shows that with terms *II*, *III* and *IV* combined to one term is similar to a temperature dependent source term in a 2-D transient heat conduction equation. In the present work, Eq. (1) is numerically solved using the FVM [23]. In the FVM approach, Eq. (1) is first integrated over the discrete time $\Delta t$ and the control volume $\Delta V = \Delta x \times \Delta y$

$$\int_t^{t+\Delta t}\left(\int_{\Delta V} \rho c_p \frac{\partial T}{\partial t} dV\right) dt = \int_t^{t+\Delta t}\left(\int_{\Delta V} \frac{\partial\left(k\frac{\partial T}{\partial x}\right)}{\partial x} dV\right) dt + \int_t^{t+\Delta t}\left(\int_{\Delta V} \frac{\partial\left(k\frac{\partial T}{\partial y}\right)}{\partial y} dV\right) dt + \int_t^{t+\Delta t}\left(\int_{\Delta V}\left(\eta_b \rho_b c_{pb}\left(T_a - T\right) + Q_m + Q_s\right) dV\right) dt. \tag{2}$$

With reference to Fig. 2a and b, in discrete form, Eq. (2) is written as

$$T_P^{n+1} = T_P^n + \frac{\Delta t\, k}{\rho c_p (\Delta x)^2}\left(T_E^n - 2T_P^n + T_W^n\right) + \frac{\Delta t\, k}{\rho c_p (\Delta y)^2}\left(T_N^n - 2T_P^n + T_S^n\right) + \frac{\Delta t}{\rho c_p}\left[\eta_b \rho_b c_{pb}\left(T_a^n - T_P^n\right) + Q_m + Q_s\right] \tag{3}$$

where temperature $T$ with suffix $P$ is the volume averaged value at the center of the discrete control volume (Fig. 1c), and those with suffixes $E$, $W$, $N$ and $S$ are the same at its east, west, north and south neighboring nodes. In Eq. (3), $n$ represents the time level.

Apart from the four boundary conditions, the solution of Eq. (3) requires an initial condition. At all nodes, the temperature at $n = 0$th level is taken as the effective local heat source temperature $T_e$ given by,

$$T_e = T_a + \frac{Q_m + Q_s}{\rho_b \eta_b c_{pb}}. \tag{4}$$

With thermophysical properties known, and the initial and the boundary conditions as stated above, Eq. (3) is solved to obtain the steady-state temperature distribution of a tissue with and without a tumor. The solver is first validated against the results available in the literature [13]. Breast is a 3-D tissue. However, in the present work, the tissue has been considered to be a mathematically 2-D one. To justify this usage, next temperature distributions from 3-D and 2-D breast tissues are compared. Having justified the usage of the 2-D tissue, spatial temperature profiles of the skin are obtained for different sizes and locations of the tumor. The similar spatial temperature profiles then become the basis of estimation of the size and locations of the tumor in the inverse analysis.

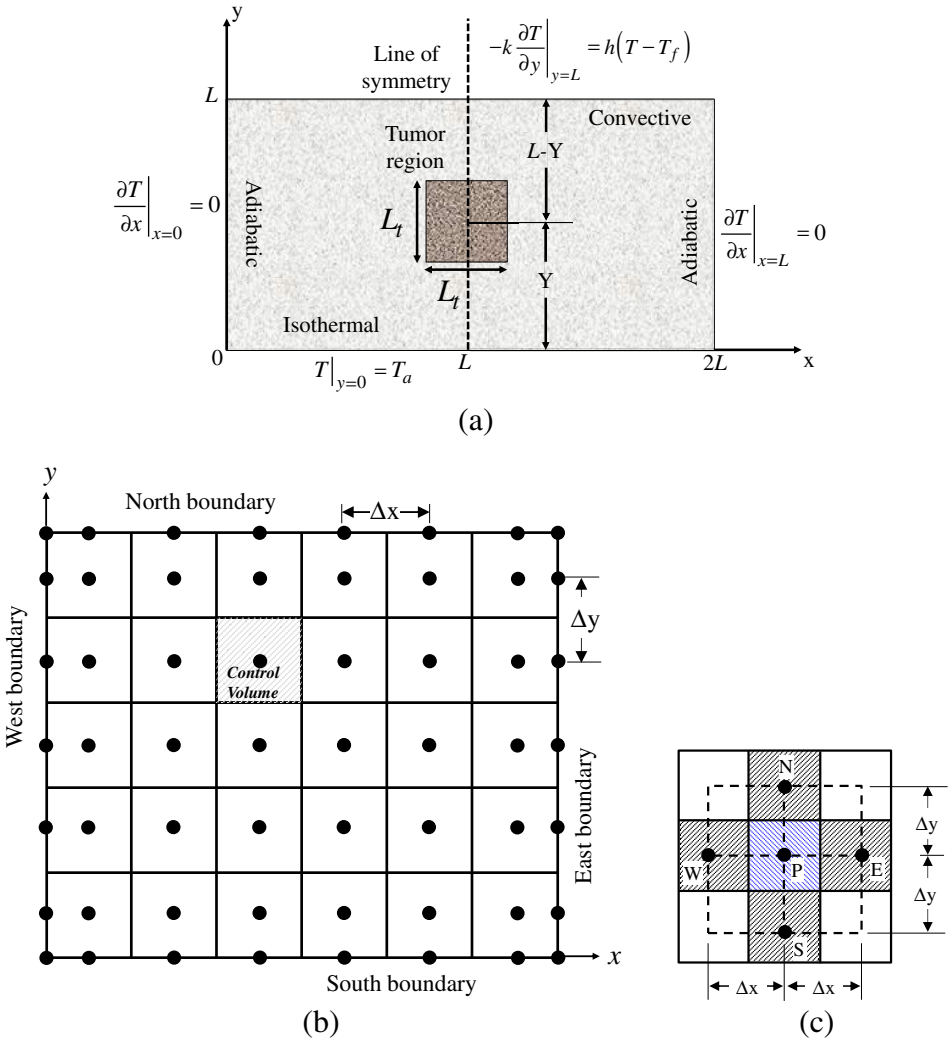


**Fig. 1.** Schematic of (a) 2-D tissue with a tumor, showing the boundary conditions, (b) 2-D discretized space and (c) control volume used in the FVM.

## 3. Results and discussion

For the two grades of the centrally located tumor, the steady-state temperature distributions on the skin surface ($x$, $L$) and along the centerline ($L$, $y$) are compared against the results of Zhang [13] in Fig. 3a and b, respectively. For these validations, with $L = 5.0$ cm, the bottom boundary ($0 \le x \le 2L, y = 0$) is at the core body temperature of 37 °C. The skin surface ($0 \le x \le 2L, y = L$) is exposed to the convective condition with $h = 20\ \mathrm{Wm^{-1}K^{-2}}$ and $T_f = 20$ °C. The left ($x = 0$, $0 \le y \le L$) and the right ($x = 2L$, $0 \le y \le L$) boundaries of the tissue are adiabatic. A tumor of size ($\frac{L}{4} \times \frac{L}{4}$) is located at the center of the domain (Fig. 1a). The thermo-physical properties used are [13]: thermal conductivity $k = 0.5\ \mathrm{Wm^{-1}K^{-1}}$, densities of the tissue and the blood $\rho = \rho_b = 1052\ \mathrm{kg\ m^{-3}}$, the specific heats of the tissue and the blood, $c_p = c_{pb} = 3800\ \mathrm{J\ kg^{-1}K^{-1}}$, for the normal tissue blood perfusion rate $\eta_b = 1 \times 10^{-4}\mathrm{s^{-1}}$ and the metabolic heat generation rate, $Q_m = 400\ \mathrm{W\ m^{-3}}$. Blood perfusion rate and the metabolic heat generation rates are: tumor I – ($\eta_b = 1 \times 10^{-3}\ \mathrm{s^{-1}}$, $Q_m = 4000\ \mathrm{W\ m^{-3}}$) and tumor II – ($\eta_b = 1 \times 10^{-2}\ \mathrm{s^{-1}}$, $Q_m = 40000\ \mathrm{W\ m^{-3}}$). Distributed volumetric heat source due to spatial heating $Q_s$ is considered absent.

As the geometry (Fig. 1a) is symmetric about the line ($L$, $y$), for the purpose of computation, consideration is given to the right hand part of it. The left hand boundary of the computational domain hence has a symmetry boundary condition i.e., adiabatic. In order to obtain a grid independent solution, the computational domain ($L \le x \le 2L$, $0 \le y \le L$) is divided into $50 \times 50$ control volumes, with time step $\Delta t$ as 0.01 s. Steady-state skin surface ($x$, $L$) and centerline ($L$, $y$) temperature distributions are compared against the results of Zhang [13] (2008) in Fig. 3a and b, respectively obtained using the lattice Boltzmann method. The results are further compared against that obtained by solving the same problem using finite element method (FEM) based-solver, COMSOL 4.3a. For the tissue, with and without tumors, temperature distributions obtained using the FVM and the FEM show a good match with the results of Zhang [13] (Fig. 2). In the absence of the tumor, at the steady-state, temperature (27.77 °C) along the skin surface is constant (Fig. 2a), while, in the presence of a tumor, throughout the skin surface, temperature rises. Temperature rise is the maximum in the center ($L$, $L$) of the skin, and it continuously decreases away from it. Temperature rise at any location on the skin is more for the tumor II for which the blood perfusion rate and metabolic heat generation rate are higher than that for the tumor I. With increase in blood perfusion rate, more heat is taken away from the tumor region, and this causes reduction in temperature. On the other hand, with increase in metabolic heat generation rate, more heat is generated and this increases the temperature. As the tumor advances, the metabolic heat generation rate becomes very high, and it not only nullifies the effect of blood perfusion, but also contributes further to the temperature rise.

Consideration of a 2-D rectangular domain in the present work is a numerical simplification to a realistic 3-D human breast. In order to

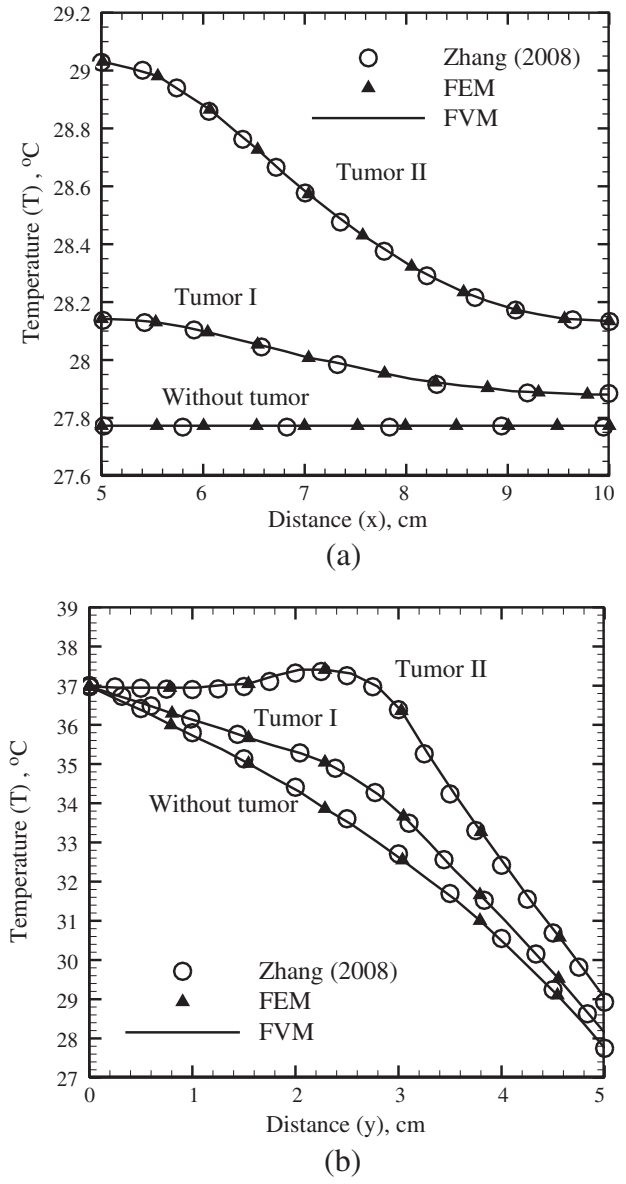


**Fig. 2.** Comparison of steady-state temperature distribution obtained using FVM and FEM along (a) the skin surface ($x$, $L$) and (b) the centerline ($L$, $y$) with Zhang [13].

find out the extent of closeness of the simplification, a hemispherical model of the breast as shown in Fig. 3a is considered. The hemisphere of radius $r = 10.0$ cm is having a spherical tumor of radius ($r_t$) 1.5 cm, which is located at a depth of 2 cm from the skin along the negative $y$-direction. For the healthy breast tissue, the blood perfusion rate and the metabolic heat generation rate considered are $0.92 \times 10^{-3}$ $s^{-1}$ and 450 $Wm^{-3}$, respectively. In case of the spherical tumor, the value of these properties is taken as $4.5 \times 10^{-3}$ $s^{-1}$ [24] and 29,000 $Wm^{-3}$ [25], respectively. Other properties of the tissue and the blood taken are the same as the earlier case [13]. The flat surface ($xz$ − plane) of the hemisphere is at isothermal core body temperature of 37 °C, whereas the curved skin surface is exposed to a convective environment with $h = 20$ $Wm^{-2}K^{-1}$ and $T_f = 20$ °C. These core body and convective conditions are the same as that for the case considered before for the validation (Fig. 3a and b).

The 2-D counterpart of the 3-D model (Fig. 3a) of the breast with a tumor is mathematically taken as a rectangular domain with a square shaped tumor (Fig. 3b). The 2-D domain is considered to be on the $xy$-plane (Fig. 3a) with a length of 10 cm (=r) and a width of 31.41 cm (=$\pi r$), and the $y$-axis is the line of symmetry. The spherical tumor is reduced to a 2-D square shaped tumor of size $L_t$ located at 8 cm from the surface. Considering equal area covered by both the geometries of the tumor on the $xy$-plane, the value of $L_t$ is found from the relation $L_t^2 = \pi r_t^2$. The boundary of the 2-D domain lying over the $x$-axis is considered at isothermal condition of 37 °C and the boundaries normal to $x$-axis are taken as adiabatic. The boundary which is parallel to $x$-axis and at a distance $r$ is kept at the same convective condition as that for the 3-D model. With all the system properties and the boundary conditions provided, Pennes bioheat equation is solved numerically using the FEM for the 3-D domain (Fig. 3a), and the FVM is used for the 2-D domain (Fig. 3b) of the breast tissue. Fig. 3c and d show the comparisons of the steady-state temperature distribution along the $y$-axis (centerline) and along the skin surface in a breast tissue with and without tumor for 2-D and 3-D models, respectively. The results from the actual 3-D and the simplified 2-D models obtained using different methods compare exceedingly well for the centerline temperature profile, whereas the 2-D geometry estimates the skin surface temperature approximately 0.5 °C higher than that of the 3-D model and hence, justifies the use of the simplified geometry.

Validation of the developed solver and the closeness of the simplified 2-D rectangular geometry with the 3-D one makes it appropriate for application to the realistic breast. For a healthy breast tissue, the blood perfusion rate and the metabolic heat generation rate are $\eta_b = 0.92 \times 10^{-3}$ $s^{-1}$ and $Q_m = 450$ $Wm^{-3}$, respectively; while, in cancerous condition, the value of the blood perfusion rate lies in the range of $\eta_b = 1.22 \times 10^{-3} - 14.5 \times 10^{-3} s^{-1}$ with a mean of $\eta_b = 4.9 \times 10^{-3}$ $s^{-1}$ [24]. A high value of the metabolic heat generation rate of 29,000 $Wm^{-3}$ [25] is observed for a cancerous tumor of breast. With other thermophysical properties of the tissue taken as $k = 0.42$ $Wm^{-1}K^{-1}$, $\rho = 920$ kg $m^{-3}$ and $c_p = 3000$ J $kg^{-1}K^{-1}$, [25] the effect of location (Y) of different sizes of the tumor on the temperature profile is studied. The properties of the blood considered are: $\rho_b = 1052$ kg $m^{-3}$ and $c_{pb} = 3800$ J $kg^{-1}K^{-1}$.

For a centrally located tumor of size 0.5 cm and 2.5 cm, effect of location (L − Y) of the tumor on the steady-state skin surface temperature distributions are shown in Fig. 4a and b, respectively. For these and subsequent results, computations are done for the entire domain. At the steady-state, in the absence of a tumor, a healthy tissue yields uniform skin surface temperature of 31.34 °C. When a tumor is present, the skin surface temperature increases, and the uniformity is lost. For any location or any size, the skin surface temperature profiles are similar, and their spatial distribution is Gaussian in nature.

An observation of Fig. 4a and b reveals that when the distance ($L$ − Y) of the tumor from the skin surface decreases, temperature of the skin increases. For a tumor of size 0.5 cm × 0.5 cm, when the distance ($L$ − Y) of the center of the tumor are 4.5 cm, 1.75 cm and 0.75 cm, the increase in the peak temperature at ($L$, $L$) are 0.001, 0.09 and 0.56 °C, respectively (Fig. 4a). While for the tumor with 2.5 cm, when the distances ($L$ − Y) of the center of the tumor are 3.25 cm, 2.75 cm, 2.25 and 1.75 cm, the increase in peak temperature at ($L$, $L$) is 0.18, 0.365, 0.77 and 1.7 °C, respectively (Fig. 4b). Another important observation from the skin surface temperature distributions shown in Fig. 4 a and b is that when the distance ($L$ − Y) of the tumor from the skin surface decreases, the peak magnitude (amplitude $A$) of the skin surface temperature profile increases. When ($L$ − Y) → $L$, i.e., the tumor is far away from the skin surface, the amplitude $A \to 0$. Similarly, with the increase in the size of the tumor, both amplitude $A$ and area under the curve increase (Fig. 4c). This increase is for the fact, when the size of the tumor increases, the heat generated also increases. The effect is clearly visible from a comparative plot of the steady-state temperature distributions for various sizes of the tumor located at ($L$ − Y) = 2.75 cm (Fig. 4c).

For a centrally ($x = L$) located tumor, irrespective of its size and location, it is observed from Fig. 4a–c that the spatial distribution of

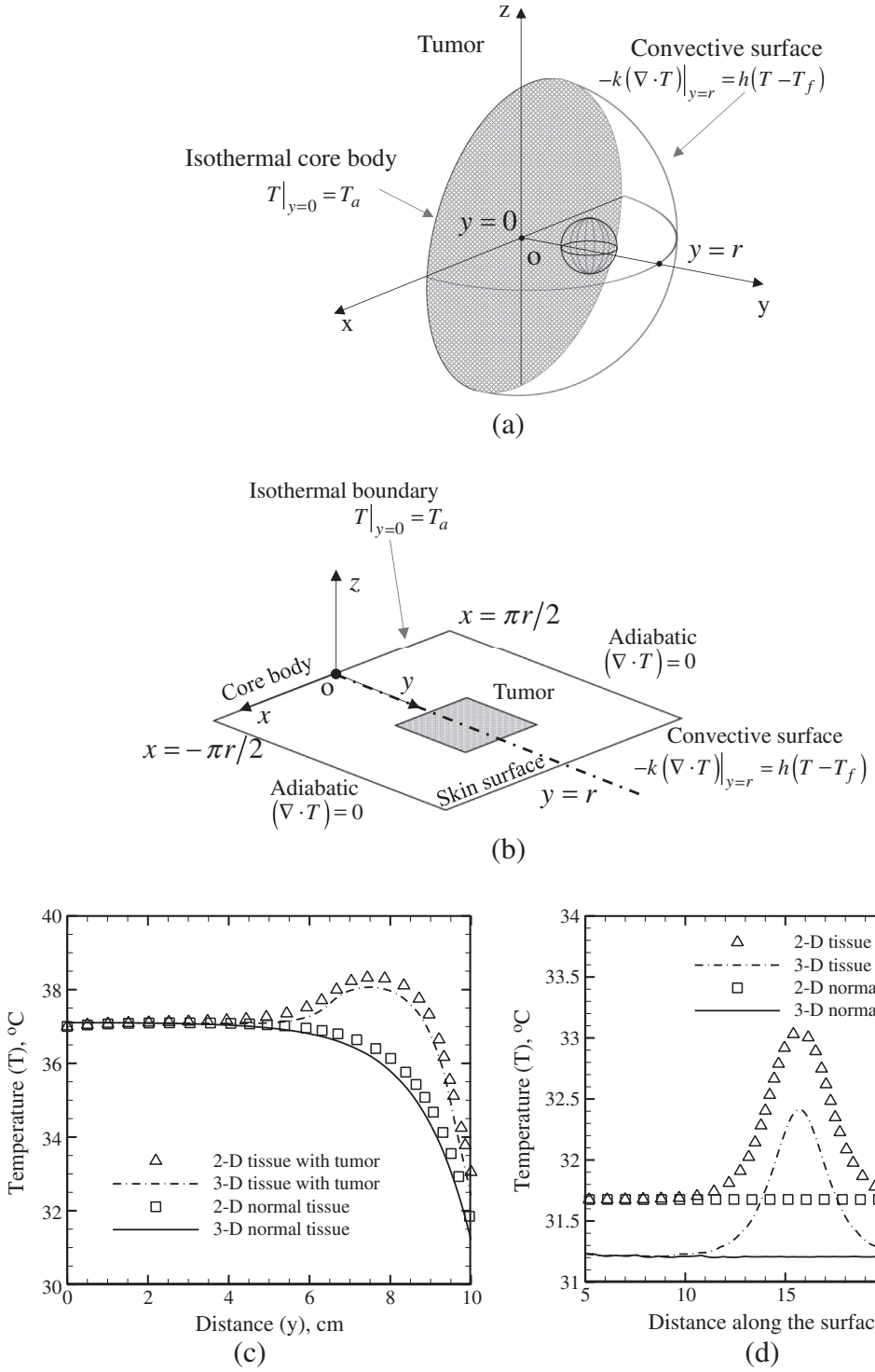


**Fig. 3.** (a) Schematic of a 3-D hemispherical breast with an imbedded tumor, (b) 2-D equivalent system of the 3-D model and steady-state (c) centerline ($L$, $y$) and (d) surface temperature distribution.

the skin surface temperature is Gaussian (Fig. 5a). The characteristics of the Gaussian profile such as the amplitude $A$, full width at half maximum (FWHM) and width $w$ (Fig. 5a) are functions of tumor size and location. With $T_o$ as the reference (base) temperature, in terms of amplitude $A$, distance $L$ and width $w$, it can be expressed as

$$T = T_o + Ae^{-(x-L)^2/2w^2}. \quad (5)$$

A tissue with a tumor of particular size and location yields a skin surface temperature profile which remains unique to that particular size and location. Hence, the amplitude, the width and the area under the curve also remain unique. In the present work, this feature is used in the proposed inverse technique to estimate the size and the location of a tumor in a tissue.

The inverse estimation of the size and the location of the tumor in a breast tissue starts with building a database of amplitude $A$ vs. location

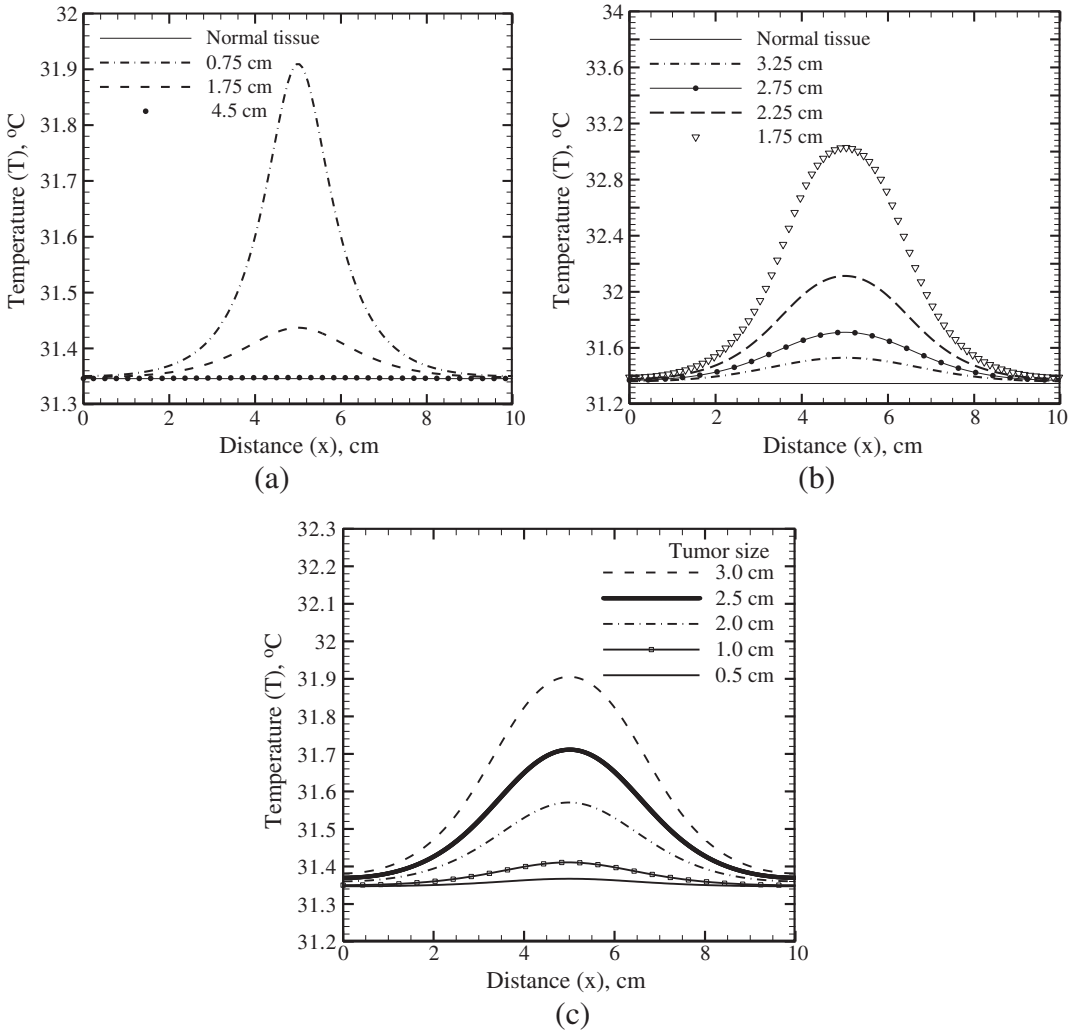


**Fig. 4.** Steady-state skin surface $(x, L)$ temperature distribution: Effect of locations $(L - Y)$ of tumor for tumor of size (a) 0.5 cm and (b) 2.5 cm, and (c) effect of sizes of the tumor located at $(L - Y) = 2.75$ cm.

Y, and area vs. location Y for different sizes of the tumor. For an unknown condition of the tissue, the obtained surface temperature profile is fitted with a curve fitting tool using a Gaussian fit. The amplitude of the curve so obtained is searched in the stored database of A vs. Y and its corresponding size and location are noted down. Any unavailable data is interpolated from the known values. Now, from the database of area vs. Y, for that particular size, at that location, the area is found out. The match of the found area below 10% confirms the presence of a tumor of that size at that particular location. In case of any mismatch (>10%), the search process continues till the end of the database. The developed solver performs different operations such as search, interpolation and matching of values, etc.

With the proposed technique, a database of amplitude $A$ vs. location Y is made for 0.5 cm, 1.0 cm, 2.0 cm, 2.5 cm and 3.0 cm of the tumors with the mean value of blood perfusion rate. For the given size of the tumor, another database of the values of area vs. location (Y) is made. The uniqueness of the skin surface temperature profiles can be made clear from the profiles of area and amplitude against the location Y, for different sizes of the tumor as shown in Fig. 5b and c, respectively. As the blood perfusion rate of a breast tumor varies over a small range of $1.22 \times 10^{-3} - 14.5 \times 10^{-3} s^{-1}$ [24], very minor change in the steady state temperature profile is observed even for the limiting values of $\eta_b$ (Fig. 5d). Hence, the database can be made using any value of $\eta_b$ within the range. In this case, the mean value of blood perfusion rate $4.9 \times 10^{-3} s^{-1}$, as reported in the literature [25], is considered for the purpose.

Steady-state skin surface temperature profile of a breast with and without a tumor obtained from measurement serves as the reference temperature profile. In the present case, however, numerically computed skin surface temperature profile obtained by solving the Pennes bioheat equation serves this purpose. This temperature profile is fitted in a curve fitting tool using Gaussian fit, and the values of its amplitude and area are obtained, and these are fed to the solver. After going through the series of operations as stated before, when the match is within the set value (≤10%), the estimation of the size and location of the tumor is assumed to be complete.

Table 1 shows the results of simultaneous estimation of size and location of 25 different sizes and locations of the tumors. In practice, in the proposed approach while doing the estimation, nothing else but the skin surface temperature profile is needed that gives its amplitude and area. Knowledge about the thermophysical properties, the blood perfusion rate and the metabolic heat generation rate are not needed. An observation of results in Table 1 shows that in most of the cases, size and location are exactly estimated. In some cases, the maximum error in estimation of the size is 4.167%, while the same in location is 7.7%. Though this accuracy in estimation is accepted, this accuracy can further be refined by making the database comprehensive by considering wide ranges of sizes and locations of the tumor.

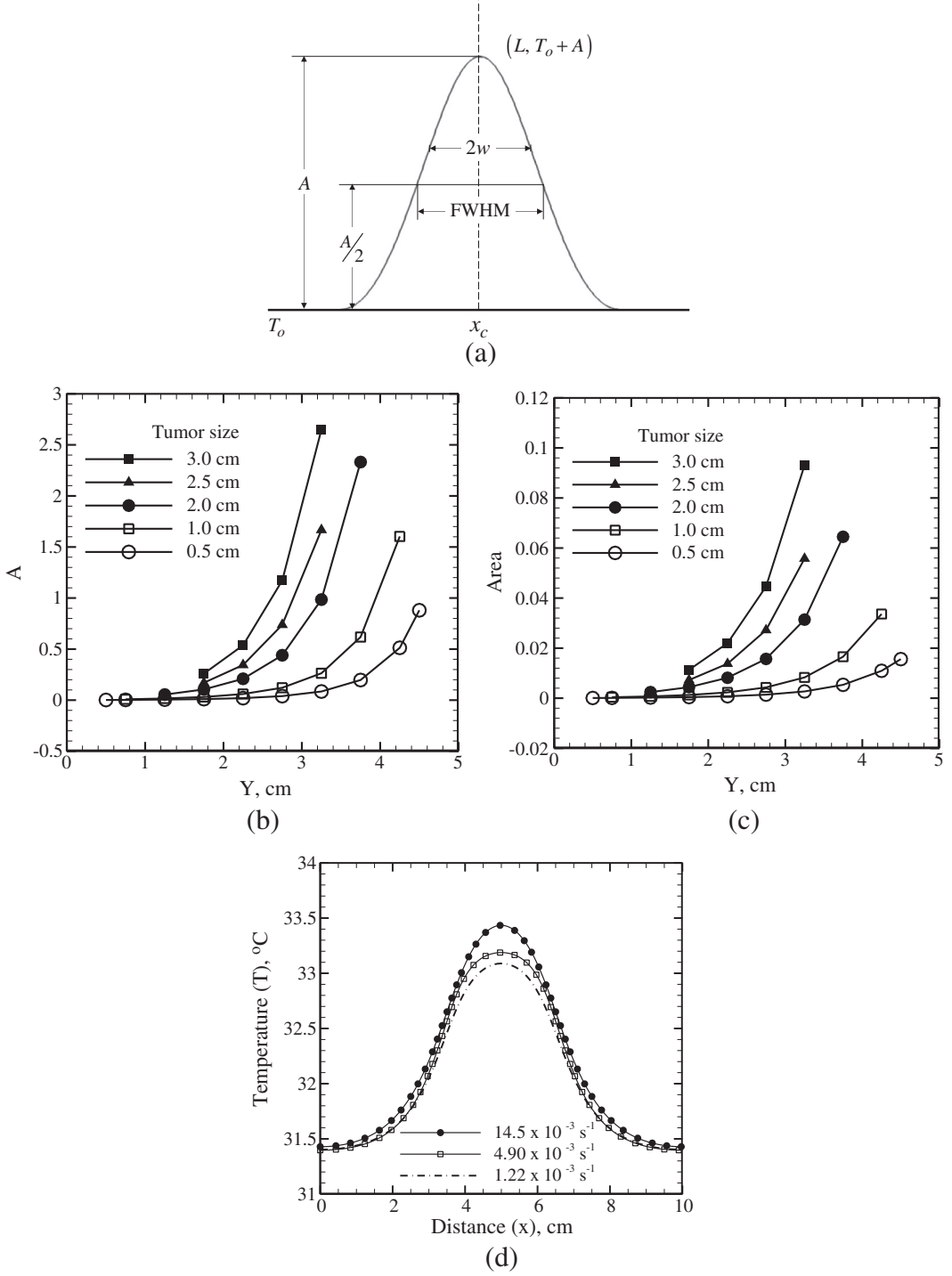


**Fig. 5.** (a) Schematic of a Gaussian profile, and variation of its (b) amplitude and (c) area for different sizes of tumors at its different locations $Y$ in a 2-D tissue with (d) effect of change of blood perfusion rate ($\eta_b$) on steady-state skin surface ($x$, $L$) temperature distribution for a tumor of size 3 cm located at $Y = 3.0$ cm.

The optimization tools like the genetic algorithm (GA), used in the inverse analysis are time consuming [17]. In GA, the unknown parameters of the system are assigned random values to the population within the defined range; and the fitness (objective) function, $J = \sum_{i=1}^{N_x} \left(T_{i,N_y}^{\text{ref}} - T_{i,N_y}\right)^2$ is to be minimized. Here, $T_{i,N_y}^{\text{ref}}$ is the skin surface temperature obtained from measurement (fixed) and $T_{i,N_y}$ has to be calculated using the values (random value at first time) of unknown parameter. The values of the parameters are changed using various tools of the GA, such as reproduction, crossover and mutation in such a way that $T_{i,N_y}$ is pushed towards $T_{i,N_y}^{\text{ref}}$ by minimizing $J$. Calculation of $T_{i,N_y}$ using the unknown parameters, for every member of the population and for each generation, needs solution of Eq. (1), i.e., the inverse analysis using the GA requires solution of the direct problem. This makes the process time consuming. However, in the proposed approach, the database has to be made using direct method only once. Each time, while using the inverse solver, the direct formulation need not have to be evaluated. Simply by searching, sorting

**Table 1**
Inverse estimated value of location and size of a tumor in 2-D breast tissue.

| Sl no. | Blood perfusion rate × $10^3$ | Actual value | | Estimated value | | Error (%) | |
|---|---|---|---|---|---|---|---|
| | | Size, $L_t$ (cm) | Location, Y (cm) | Size, $L_t$ (cm) | Location, Y (cm) | Size, $L_t$ | Location, Y |
| 1 | 4.9 | 0.48 | 4.25 | 0.50 | 4.25 | 4.167 | 0.000 |
| 2 | 4.9 | 0.49 | 4 | 0.5 | 3.9328 | 2.041 | 1.680 |
| 3 | 4.9 | 0.50 | 1.250 | 0.50 | 1.250 | 0.000 | 0.000 |
| 4 | 4.9 | 0.50 | 3.816 | 0.50 | 3.779 | 0.000 | 0.962 |
| 5 | 2 | 0.50 | 1.250 | 0.50 | 1.328 | 0.000 | 6.232 |
| 6 | 10 | 0.50 | 4.000 | 0.50 | 4.102 | 0.000 | 2.557 |
| 7 | 14.5 | 0.51 | 3.250 | 0.50 | 3.335 | 1.961 | 2.604 |
| 8 | 10.5 | 0.52 | 3.250 | 0.50 | 3.315 | 3.846 | 1.988 |
| 9 | 4 | 0.98 | 3.500 | 1.00 | 3.403 | 2.041 | 2.766 |
| 10 | 4 | 0.99 | 4.000 | 1.00 | 3.889 | 1.010 | 2.788 |
| 11 | 4.9 | 1.00 | 1.750 | 1.00 | 1.784 | 0.000 | 1.949 |
| 12 | 4.9 | 1.00 | 2.790 | 1.00 | 2.783 | 0.000 | 0.251 |
| 13 | 3.5 | 1.00 | 4.000 | 1.00 | 3.895 | 0.000 | 2.620 |
| 14 | 5.67 | 1.00 | 1.000 | 1.00 | 0.922 | 0.000 | 7.770 |
| 15 | 4.9 | 2.00 | 2.750 | 2.00 | 2.750 | 0.000 | 0.000 |
| 16 | 4.9 | 2.00 | 1.260 | 2.00 | 1.250 | 0.000 | 0.762 |
| 17 | 3.55 | 2.00 | 3.750 | 2.00 | 3.718 | 0.000 | 0.843 |
| 18 | 7.58 | 2.00 | 3.000 | 2.00 | 2.932 | 0.000 | 2.277 |
| 19 | 4.9 | 2.50 | 1.750 | 2.50 | 1.750 | 0.000 | 0.000 |
| 20 | 4.9 | 2.50 | 3.000 | 2.50 | 2.946 | 0.000 | 1.787 |
| 21 | 6.8 | 2.50 | 2.800 | 2.50 | 2.772 | 0.000 | 0.993 |
| 22 | 4.9 | 3.00 | 3.250 | 3.00 | 3.250 | 0.000 | 0.000 |
| 23 | 4.9 | 3.00 | 1.800 | 3.00 | 1.784 | 0.000 | 0.883 |
| 24 | 5.5 | 3.00 | 2.100 | 3.00 | 2.034 | 0.000 | 3.167 |
| 25 | 3.95 | 3.00 | 3.000 | 3.00 | 2.949 | 0.000 | 1.697 |

and interpolating from the database with the reference parameters (*A* and *Area*), the size and location are estimated which makes the computation exceedingly fast. For the present geometry, with 100 × 100 control volumes, the genetic algorithm with population size 1000 on 32 bit-2.10 GHz processor with 2 GB RAM took almost 16 h, while the proposed approach, the estimation has been instantaneous. It took less than 0.1 s.

## 4. Conclusions

The size and the location of a tumor inside a breast were simultaneously estimated. Estimation was based on the skin surface temperature distribution. Solution of the Pennes bioheat equation provided the skin surface temperature distribution. Use of the mathematically 2-D rectangular geometry instead of a 3-D hemispherical geometry was justified. For different sizes and locations of the tumors, the skin surface temperature distributions had Gaussian profile. The obtained Gaussian temperature profile was specific for the specific size and location of the tumor. The characteristics of the Gaussian temperature profile, viz., the amplitude and the area were the basis of estimation using the proposed curve fitting technique. Estimations were done for a wide range of values of size and locations. The size and the location of the tumor were estimated with good accuracy. The analysis of the estimation was not only simple; the required computational time was almost insignificant compared to the estimation of the same parameters using the genetic algorithm.

## References


[1] National Cancer Institute, www.cancer.gov/ (retrieved on 2 October 2013).
[2] GLOBOCAN, http://globocan.iarc.fr/factsheet.asp (retrieved on 28 September 2013).
[3] National Cancer Foundation, http://www.nationalbreastcancer.org (retrieved on 28 September 2013).
[4] G.E. Byrns, K.H.P. Ciacco, L.A. Shands, K.P. Fennelley, C.S. McCammon, A.Y. Boudreau, P.N. Breysse, C.S. Mitchell, Chemical hazards in radiology, Appl. Occup. Environ. Hyg. 15 (2000) 203–208.
[5] H.H. Pennes, Analysis on tissue arterial blood temperature in the resting human forearm, J. Appl. Physiol. 1 (1948) 93–122.
[6] A.V. Kuznetsov, Optimization problems for bioheat equation, Int. Commun. Heat Mass Transf. 33 (2006) 537–543.
[7] P. Keangin, P. Rattanadecho, T. Wessapan, An analysis of heat transfer in liver tissue during microwave ablation using single and double slot antenna, Int. Commun. Heat Mass Transf. 38 (2011) 757–766.
[8] M.S. Ferreira, J.I. Yanagihara, A heat transfer model of the human upper limbs, Int. Commun. Heat Mass Transf. 39 (2012) 196–203.
[9] Ping Yuan, Shin-Bin Wang, Hsien-Ming Lee, Estimation of the equivalent perfusion rate of Pennes model in an experimental bionic tissue without blood flow, Int. Commun. Heat Mass Transf. 39 (2012) 236–241.
[10] H. Ahmadikia, R. Fazlali, A. Moradi, Analytical solution of the parabolic and hyperbolic heat transfer equations with constant and transient heat flux conditions on skin tissue, Int. Commun. Heat Mass Transf. 39 (2012) 121–130.
[11] E.H. Wissler, Pennes' 1948 paper revisited, J. Appl. Physiol. 85 (1998) 35–41.
[12] K.N. Rai, S.K. Rai, Effect of metabolic heat generation and blood perfusion on the heat transfer in the tissues with a blood vessel, Heat Mass Transf. 35 (1999) 75–79.
[13] H. Zhang, Lattice Boltzmann method for solving bioheat equation, Phys. Med. Biol. 53 (2008) N15–N23.
[14] J. Okajima, S. Maruyama, H. Takeda, A. Komiya, Dimensionless solutions and general characteristics of bioheat transfer during thermal therapy, J. Therm. Biol. 34 (2009) 377–384.
[15] P.K. Gupta, J. Singh, K.N. Rai, Numerical simulation for heat transfer in tissues during thermal therapy, J. Therm. Biol. 35 (2010) 295–301.
[16] K. Das, R. Singh, S.C. Mishra, Numerical analysis for determination of the presence of a tumor and estimation of its size and location in a tissue, J. Therm. Biol. 38 (2013) 32–40.
[17] K. Das, S.C. Mishra, Estimation of tumor characteristics in a breast tissue with known skin surface temperature, J. Therm. Biol. 38 (2013) 311–317.
[18] J.H. Zhou, J Liu, Numerical study on 3-D light and heat transport in biological tissues embedded with large blood vessels during laser-induced thermotherapy, Numer. Heat Transf. A 45 (2004) 415–449.
[19] R. Muthukumaran, S.C. Mishra, Radiative transfer of a short-pulse laser wave of Gaussian temporal profile through a 2-D participating medium containing inhomogeneities of different shapes at various locations, Numer. Heat Transf. A 54 (2008) 546–567.
[20] R. Muthukumaran, S.C. Mishra, S. Maruyama, K. Mitra, Assessment of signals from a tissue phantom subjected to radiation sources of temporal spans of the order of a nano-, a pico- and a femto-second — a numerical study, Numer. Heat Transf. A 60 (2011) 154–170.
[21] P.W. Partridge, L.C. Wrobel, An inverse geometry problem for the localization of skin tumors by thermal analysis, Eng. Anal. Bound. Elem. 31 (2007) 803–811.
[22] R. Das, S.C. Mishra, R. Uppaluri, Multi-parameter estimation in a transient conduction-radiation problem using the lattice Boltzmann method and the finite volume method coupled with the genetic algorithms, Numer. Heat Transf. A 53 (2008) 1321–1338.
[23] H.K. Versteeg, W. Malalasekera, An introduction to computational fluid dynamics, the finite volume method, Longman Group Limited, New York, 1995. 168–173.
[24] D.A. Mankoff, L.K. Dunnwald, J.R. Gralow, G.K. Ellis, A. Charlop, T.J. Lawton, E.K. Schubert, J. Tseng, R.B. Livingston, Blood flow and metabolism in locally advanced breast cancer: relationship to response to therapy, J. Nucl. Med. 43 (2002) 500–509.
[25] M. Gautherie, Thermopathology of breast cancer: measurement and analysis of in-vivo temperature and blood flow, Ann. N. Y. Acad. Sci. 335 (1980) 383–415.